

Experimental Investigation of Two Interacting Thruster-Plumes Downstream of the Nozzles

André Holz⁽¹⁾, Georg Dettleff⁽¹⁾, Klaus Hannemann⁽¹⁾ and Stefan Ziegenhagen⁽²⁾

(1) DLR-Institut für Aerodynamik und Strömungstechnik, Bunsenstrasse 10,
D - 37073 Göttingen
Andre.Holz@dlr.de

(2) Astrium GmbH, P.O. Box 11 19, D - 74215 Moeckmuehl

Abstract

The plume-plume interaction of two small cold gas thrusters is investigated under high vacuum conditions in the DLR high vacuum plume test facility STG-CT. In this paper we concentrate on the interaction downstream of the nozzles. After introducing the experimental equipment, characteristics of shock interaction are presented. Furthermore the appropriateness of the Penetration Knudsen Number for predicting the type of interaction also for thruster plumes is investigated.

Nomenclature

a	[mm]	Slit orifice height
A_P		Plume constant
d	[mm]	Slit orifice width
d_E	[mm]	Nozzle exit diameter
d^*	[mm]	Nozzle throat diameter
$f(\theta)$		Function (of θ)
\dot{n}	$\left[\frac{1}{m^2s} \right]$	Particle flux
N_2		Nitrogen
p_K	[mbar]	Pressure in Patterson probe
p_0	[mbar]	Stagnation pressure
Kn_p		Penetration Knudsen Number
l_E	[mm]	Length: nozzle throat - exit
r	[mm]	Distance: probe – nozzle
r^*	[mm]	Radius nozzle throat
T_K	[K]	Temperature converter
T_S	[K]	Temperature slit orifice
T_0	[K]	Stagnation temperature
γ		Ratio of specific heats
δ	[m]	Boundary layer thickness
λ	[m]	Mean free path
ρ	$\left[\frac{kg}{m^3} \right]$	Density
ρ^*	$\left[\frac{kg}{m^3} \right]$	Density in nozzle throat
θ	[°]	Rotation angle of thruster

1.) Introduction

In spacecraft propulsion technology a parallel arrangement of two or more thrusters is used to obtain a desired thrust range by such clustering or to perform fine thrust tuning by a combination of bigger and smaller thrusters.

As a consequence of simultaneous firing the thruster plumes will interact. In this case their impingement on neighbouring surfaces cannot be treated by a linear superposition of the single plumes (apart from the complete free molecular case). In the interaction region the flow has its own characteristics. The impingement effects like disturbing moments, heat transfer and contamination of surfaces must therefore be studied in the configuration of interacting plumes.

The objective of the present research, which was conducted in the framework of the "Propulsion 2010" Memorandum of Understanding between DLR and Astrium GmbH, is to investigate the plume-plume interaction systematically under basic fluid mechanical as well as engineering aspects. In this paper we concentrate on the interaction characteristics downstream of two small cold gas thrusters.

The single plume with its characteristics is sketched in **Figure 1**. About 90% of the mass flow are confined within the region $\theta < 30^\circ$. The rest is distributed over the wide angular range up to about $\theta = 120^\circ$. In **Figure 2** are sketched the characteristics of two parallel and equal interacting plumes. In the interaction region the gas of the two plumes changes its flow direction and is compressed, when indicated even by a compression shock.

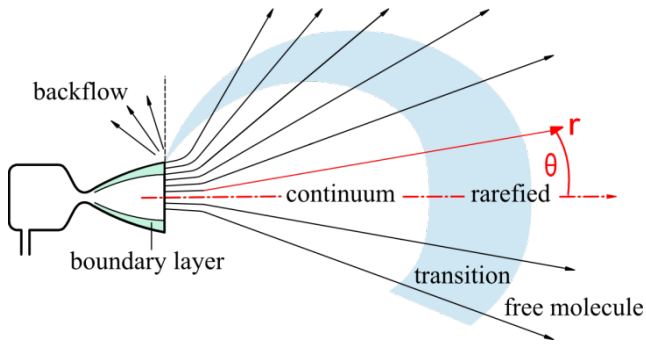


Figure 1. Single plume characteristics

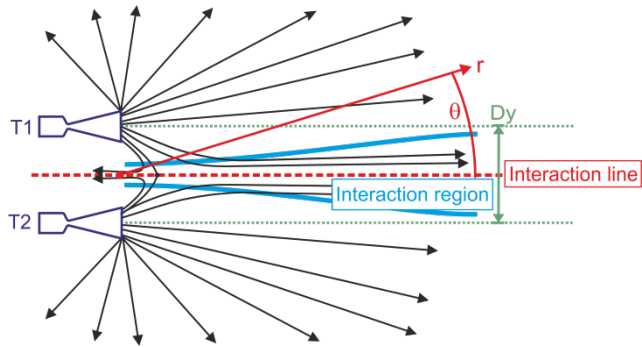


Figure 2. Plume-plume interaction characteristics

Most of the open literature deals with plume-plume interference at finite vacuum conditions in ground test facilities with noble gas sources in parallel orientation [2] [13] like in Figure 2 or counter flowing [1] [7]. The studies with parallel plumes concentrate on the shock interaction regime downstream of the shock system. The backflow regimes have not been investigated experimentally due to the lack of powerful pumping capacity.

Some numerical approaches are reported in [11] [14] [16] especially for low density conditions where the method of Direct Simulation Monte Carlo (DSMC) can be applied.

To characterize the interaction of two parallel plumes a scaling parameter, the Penetration Knudsen Number, has been introduced in [10]. In the experiments [2] [8] the plume interference occurred at high, intermediate, and low plume density levels using orifices instead of nozzles. The difference between the corresponding jets is that the flow from an orifice spreads much stronger into the off-axis region. One objective of the present study is to check the applicability of the penetration Knudsen Number concept also for thruster plumes.

The investigation was performed with two small cold gas thrusters oriented in parallel, which are driven with

gaseous Nitrogen. Such an arrangement allows varying the different relevant flow parameters in a simple way. As relevant flow parameters we consider the stagnation pressure and temperature and the gas type, characterized especially by its ratio of specific heats. In addition the type of interaction can be changed by the distance between the nozzles.

The flow field was investigated by means of a free molecular pressure probe, also called Patterson probe, by which the particle flux is measured. In [2] [8] the same probe was used.

In this paper we will first introduce the experimental equipment with the facility STG, the double-thruster testrig and the Patterson probe. After that, we have selected from our still on-going study the demonstration of the different interaction phenomena and the investigation of the Penetration Knudsen Number.

2.) Experimental setup

2.1) STG-CT

For the investigation of the interacting plume flows we have used the DLR-high vacuum plume test facility STG-CT (Figure 3). Its essential feature is a liquid-helium driven cryopump with an area of about 30 m². It encloses completely the cylindrical expansion room for the plumes with a length of 5.25 m and a diameter of 1.6 m. Even when the local heat flux is continuously 100 W/m² at a total heat load of 500 W the temperature increase of the cryopump does not exceed 0.2 K above the temperature of 4.3 K of the coolant agent. Under these conditions it is possible to generate full expansion into the highly rarefied regime at a background gas pressure below 10⁻⁶ mbar with Nitrogen as test gas. The possibility of disturbing background gas influence, for example any entrainment, is excluded.

The cryopump is enclosed by a radiation shield, which is cooled with liquid nitrogen at about 80 K to protect it from radiation heat. Both cold walls are installed in a stainless steel vacuum chamber with a length of 7.6 m and a diameter of 3.3 m. They are first cooled down to about 80 K before further cooling of the cryopump below 10 K is performed. More details can be found in [5] and [6].

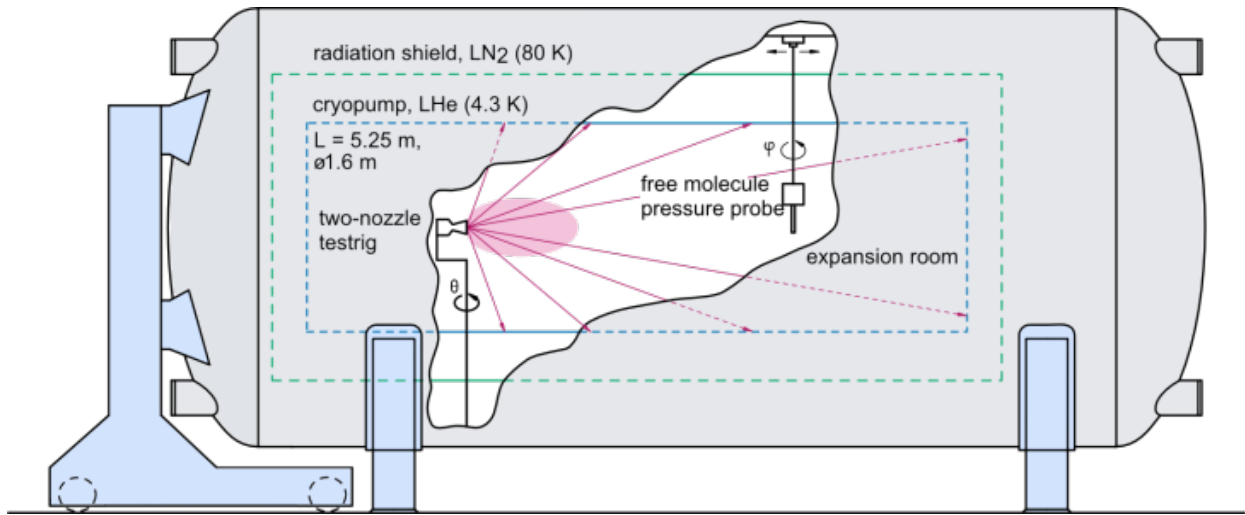


Figure 3. High vacuum plume test facility STG-CT

2.2) Two-thruster testrig

The two plumes were generated by means of two small thrusters mounted on a two-thruster rig as sketched in **Figure 4**. The test gas N_2 passes the gas supply tubes before entering the stagnation chambers where the two equal stagnation pressures p_0 and temperatures T_0 are measured. Nitrogen as test gas has a ratio of specific heats of $\gamma = 1.4$.

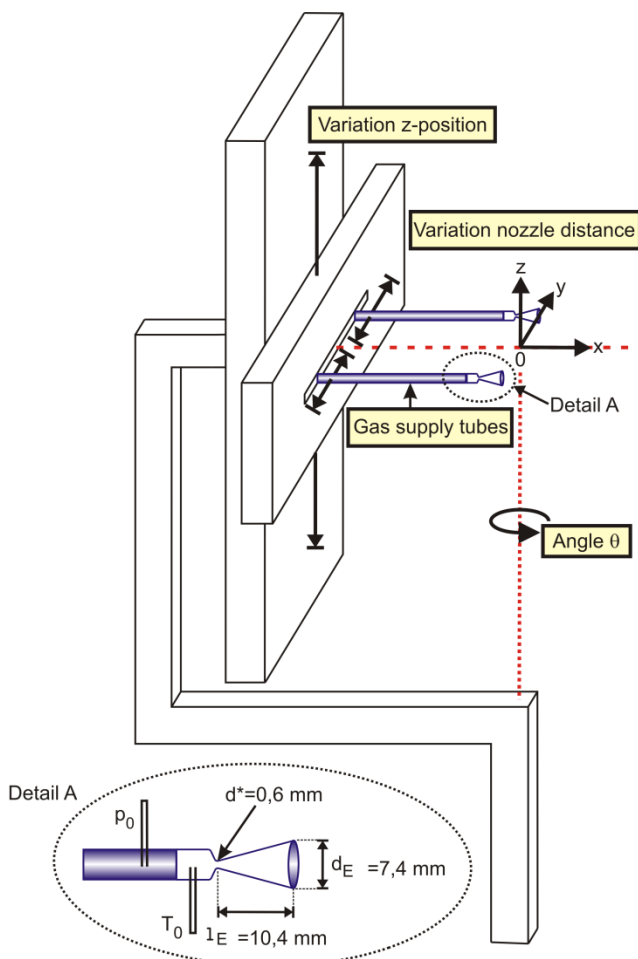


Figure 4: Two-thruster testrig

The stagnation pressures p_0 could be varied between 0.1 and 5 bar, the stagnation temperatures T_0 between 300 and 400K. In the experimental series which will be presented in the following, the stagnation conditions are:

$$p_0 = 1660 \text{ mbar and } T_0 = 300 \text{ K.}$$

The nozzles are shaped like the ones of the Astrium 10N thruster, but scaled down by a factor 4.75. Geometrical data of the nozzles can be found in **Detail A** of Figure 4.

The test rig allows to vary the distance Dy of the nozzles and thereby of the two parallel plumes, and to rotate them (also angle θ) around a vertical axis (z), which passes through the center of the connecting line of the two nozzle exits. This point is the origin of the coordinate systems, which is used for our investigation of plume-plume interaction. The thruster rig can be rotated by $\theta = 180^\circ$ around this axis. In Figure 4 is sketched a Cartesian coordinate-system. Furthermore, a system of polar coordinates r and θ is used, which is also depicted in Figure 2. Moreover the two-thruster-arrangement can be moved in the vertical z -direction. The x -axis corresponds to the interaction line, which is illustrated in Figure 2. All measurements presented in this paper are made in the x - y -plane.

In order to study directly the jet interaction each thruster gas supply can be shut by an electric valve. By running either both jets or only one, this procedure allows an easy determination of the conditions at fixed location of the single plume and then of plume interaction.

2.3) Patterson probe

To study the single plumes and the interaction characteristics of two plumes, a Patterson probe (**Figure 5a**) is installed in the chamber (Figure 3), which operates in the high pressure regime as a Pitot probe [2] and in the low density regime as a free molecular pressure probe (details for example in [9] [12]). The probe is equipped

with an ionisation pressure gauge and can measure from 10^{-6} mbar up to about 1 mbar. The slit height a is 7.5 mm and the width d is 0.8 mm. The slit is in a tube with an outer diameter of 6 mm and wall thickness of 0.5 mm. An electrical traversing system provides the movement of the probe in x -direction (Figure 4), and a probe turning mechanism allows rotating the probe around the slit orifice to $\pm 180^\circ$ (Figure 3).

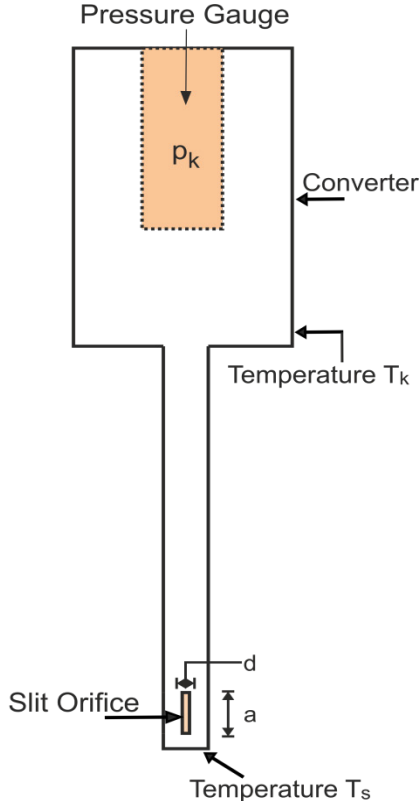


Figure 5a: Sketch of the Patterson probe

In a rarefied regime the recorded data (pressure in converter p_K , converter-temperature T_K and slit-temperature T_S) allow to determine the particle flux \dot{n} . The flow to the probe is sketched in **Figure 5b**.

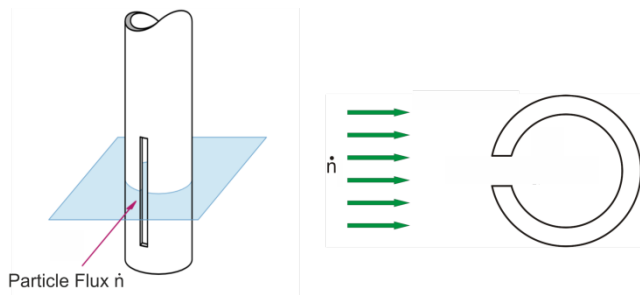


Figure 5b: Flow at the Patterson probe

The calculation of \dot{n} is based upon a theory, which was extended to flows from two sources. In the results presented here it is a sufficient approximation to assume a linear correlation between particle flux and pressure p_K . The particle flux is then given by:

$$\dot{n} = c * p_K \quad (2.3.1)$$

where c is a constant which has to be defined by measuring several profiles in which the probe is rotating

around the slit. In the following chapter, the converter pressure as a function of the probe position will always be presented, because we are mainly interested in the flow structure and qualitative character of the profiles. For calculating the particle flux the constant

$$c = 3,05 * 10^{24} \left[\frac{1}{Ns} \right] \quad (2.3.2)$$

can be used.

3.) Tests and results

3.1) Single plume

The density distribution in a single axisymmetric plume can be described analytically by a simple formula in polar coordinates (r, θ) ; Figure 1).

$$\rho(r, \theta) = \rho^* A_p f(\theta) \left(\frac{r^*}{r} \right)^2 \quad (3.1)$$

In this equation ρ is the density in the plume, ρ^* at the nozzle throat and r^* is the throat radius. The origin of the polar coordinate system is at the nozzle-exit on the centerline. Consequently, r is the distance between nozzle-exit and a location in the flow-field along a streamline, which is assumed to be straight. θ is here the angle between plume axis and streamline. A_p is a coefficient and $f(\theta)$ is a function, which describes the angular density distribution (note that $f(\theta)$ does not depend on the distance r). For both quantities various forms have been established [4]. The gas velocity is assumed to be constant with its maximum value, hence the density decrease in the far field follows the relation $\sim \frac{1}{r^2}$.

The angular density distribution $f(\theta)$ depends on geometric parameters of the nozzle, the adiabatic exponent γ of the plume gas, and the Reynolds-Number Re (which implicates dependence of the boundary layer thickness δ). By means of the Patterson Probe it will be measured $p_K \sim \dot{n}$.

In **Figure 6** we show profiles $p_K/p_{K(0^\circ)}$ measured in a plume at various distances r and normalized with their centerline value. Similarity is evident, which confirms the assumption of practically straight streamlines.

We have also marked the core region of the plume in Figure 6, which is defined by the series of inflection points of the various profiles.

Combining such points of angular profiles at different positions r leads to the straight line in **Figure 7**. Here we have plotted the core radius as a function of the profile position r . It is evident, that it increases linearly with increasing distance to the nozzle:

$$r_{core} = A + B * r \quad \text{with: } A = -8(2) \text{ mm} \\ B = 0.356(6)$$

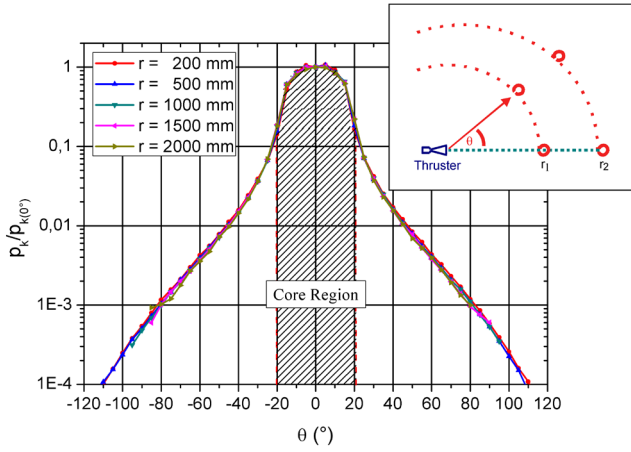


Figure 6. Angular profiles $p_K/p_{K(0^\circ)}$ at different distances r

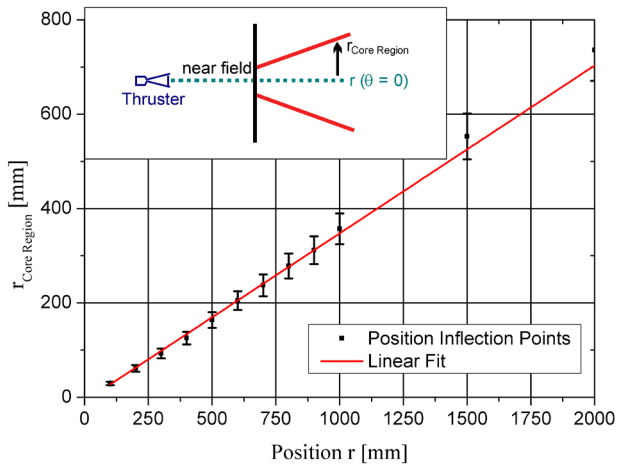


Figure 7. Radius of the core region as a function of r

We will come back to this result in the context of the plume-plume interaction in the next section.

3.2) Plume-plume interaction

In **Figure 8** we depict another illustration of the profile data $p_K(r, \theta)$ for the single plume. The interpolation was done by Tecplot 360 software [15], using the measured data as supporting points. To get a better representation by avoiding strong gradients, the logarithm of the Patterson probe pressure has been used.

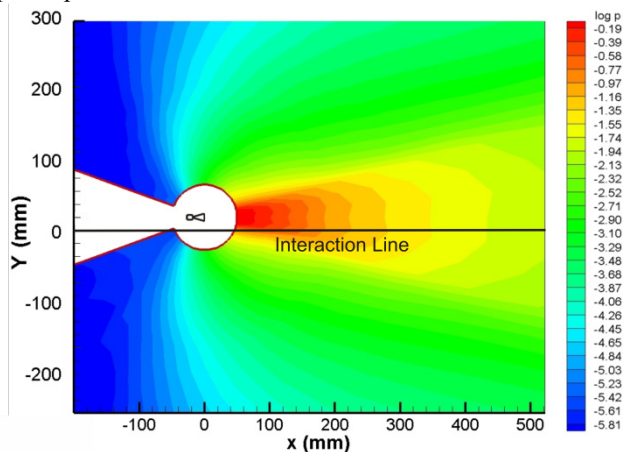


Figure 8. Flow pattern of the single plume

The cold gas thruster is placed in the center of the white circle. Within the circle the data in the core region exceeded the measurement range of 1 mbar of the pressure transducer.

The white area on the left side of the circle is marking the region, where the test rig with its gas supply, sensors, and heaters was placed. The thruster is located at $x = 0 \text{ mm} / y = 15 \text{ mm}$ within the plane $z = 0 \text{ mm}$, which we consider as interaction plane. At $y = 0 \text{ mm}$ we have indicated the interaction line. Along this line we have recorded the profile shown in **Figure 9** with only thruster 1 active.

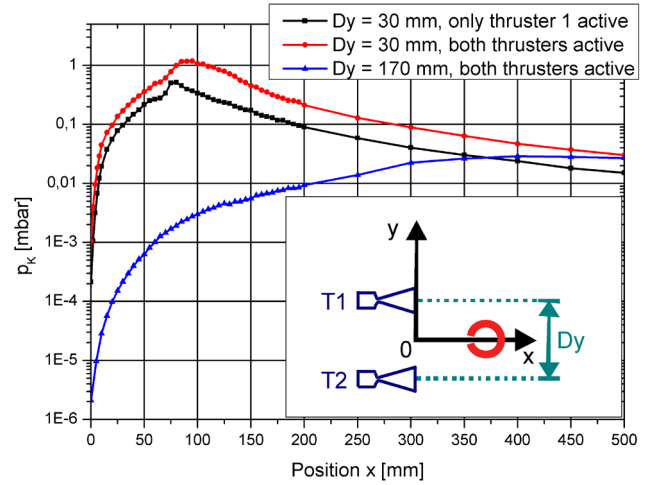


Figure 9. Radial profiles along the interaction line

The slit of the Patterson probe points to the origin of the coordinate system. Comparing **Figures 8** and **9** we find that the maximum of the curve is in the core region of the single plume. If we now place the second thruster at $x = 0 \text{ mm} / y = -15 \text{ mm}$ and fire it, we obtain the curve with both thrusters active in **Figure 9**. Their distance is $Dy = 30 \text{ mm}$.

In comparison to the black curve, the maximum has moved downstream and it is obvious, that the measured data cannot be obtained by a simple superposition of the single plume data. They exceed them considerably at some locations.

A different behavior of interaction is observed, when we increase the distance of the thrusters from 30 mm to 170 mm. Here we obtain the lower curve in **Figure 9** along the interaction line. Following the $\frac{1}{r^2}$ law, the density decreased with a factor 32, i.e. we have interaction in a more rarefied condition.

To characterize and predict the interaction quantitatively, an adapted Knudsen number, called Penetration Knudsen number Kn_p has been introduced by Koppenwallner [10]. In general the Knudsen number is given by:

$$Kn = \frac{\lambda}{l_{ref}} . \quad 3.2.$$

Here λ is the mean free path of the gas molecules and l_{ref} a reference length. Koppenwallner modified this number.

He determined the local Knudsen numbers along the interaction line, using the mean free path of the single plume gas and λ_p (indicated in the insert in **Figure 10**) as reference length. Both, λ and λ_p are not fixed, but vary along the interaction line. There is a minimum value of all these Knudsen numbers. This is called the Penetration Knudsen number. We have applied this procedure to our case of interaction and obtained the Knudsen numbers related to the angle θ , which corresponds to the location on the interaction line, as shown in Figure 10.

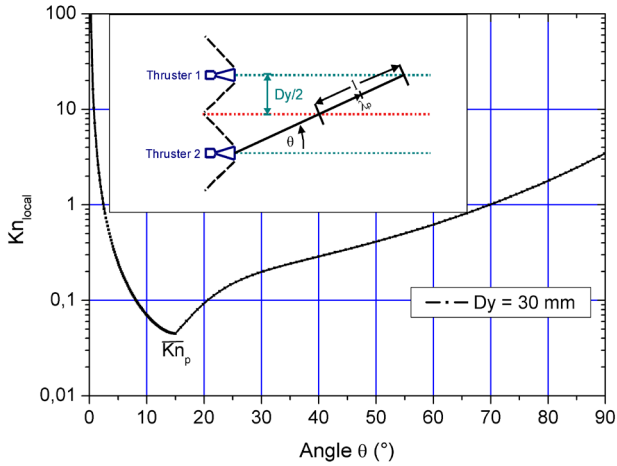


Figure 10. Penetration Knudsen number $\overline{K n_p}$ for plume-plume interaction

The minimum is defined as characteristic Penetration Knudsen number. $\overline{K n_p} = 0.045$ in this experiment. Dankert and Koppenwallner [3] found in their experiments with free jets from sonic orifices that for $\overline{K n_p} < 0.2$ the interaction region is bounded by compression waves.

We will now investigate if the interaction in our experiment is also accompanied by the formation of compression waves. They can be identified by means of angular profiles $p_K(r, \theta)$ (see Figure 2).

In **Figure 11** we show several such angular profiles for a thruster distance of $Dy = 30 \text{ mm}$ and $r = 150 \text{ mm}$. First we consider the cases thruster 1 or thruster 2 is active. The profiles are asymmetric because the origin of the coordinate system is not on the plume axis.

When both thrusters are active we obtain the profile with the two peaks, which indicate that the probe has passed compression shocks at these locations. These shocks are a clear border between the undisturbed single plumes and the interaction region. Upstream of the left shock, i.e. to the left, the single plume and the interaction profile coincide. Upstream of the right shock we find analogously the same situation. This result shows that at $\overline{K n_p} = 0.045 < 0.2$ also shocks are formed as predicted by [3] for free jets.

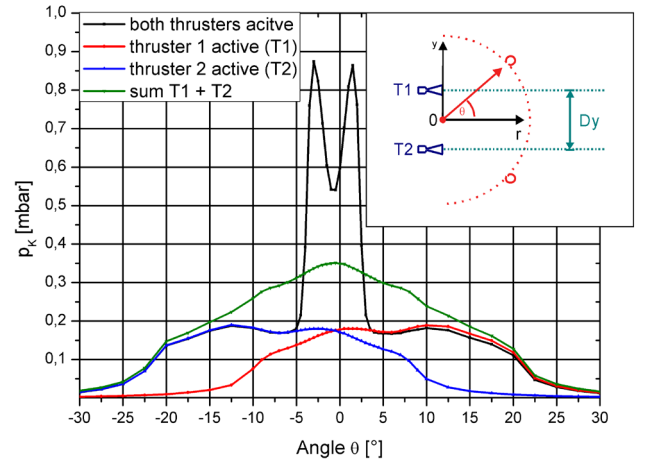


Figure 11. Angular profiles at $r = 150 \text{ mm}$, $Dy = 30 \text{ mm}$

Only for demonstration we have superposed the profiles thruster 1 active and thruster 2 active to obtain the curve sum T1+T2. Such procedure would lead to untenable results.

In **Figure 12** we show further angular profiles, determined at increasing distance r . The interaction region broadens and the pressure jump becomes smaller further downstream. The pressure along the interaction line decreases according to $p_K \sim r^{-2.3}$, i.e. faster than the density in a single plume. However, the signal p_K is composed of the product of density and velocity. It is possible that we have a varying velocity along the interaction line, because the gas at the different locations stems from different conditions behind the compression shock.

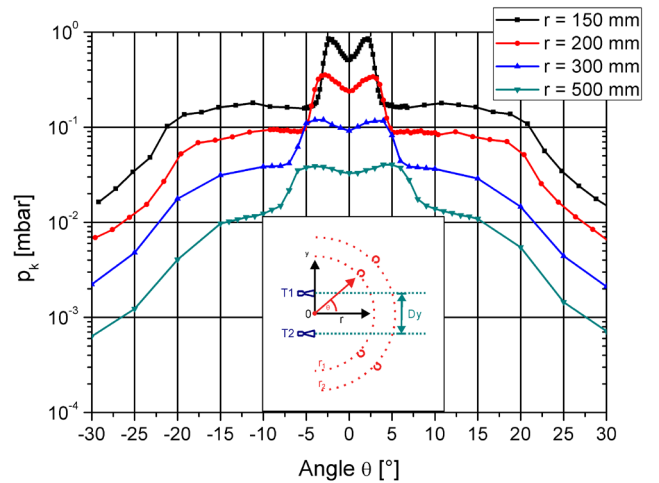


Figure 12. Angular profiles at different positions r , $Dy = 30 \text{ mm}$

Furthermore, the distance between the two shocks B is increasing with increasing r . In **Figure 13** the distance B is plotted as function of r . Within the considered region the broadening of the interaction region is linear. A fit leads to the equation:

$$B = A + B * r \quad \text{with:} \quad A = -31(1) \text{ mm} \\ B = 0.340(6)$$

By comparing this result with the development of the core radius r_{core} in section 3.1 for the single plume it is obvious

that the slopes are nearly the same (difference about 5%). We have no explanation for this surprising coincidence of the slopes in the axis-symmetric single plume and in the interaction region in the plane $z = 0 \text{ mm}$.

Apart from this coincidence the interaction flow can be interpreted as a third plume in such a configuration of two interacting thruster plumes.

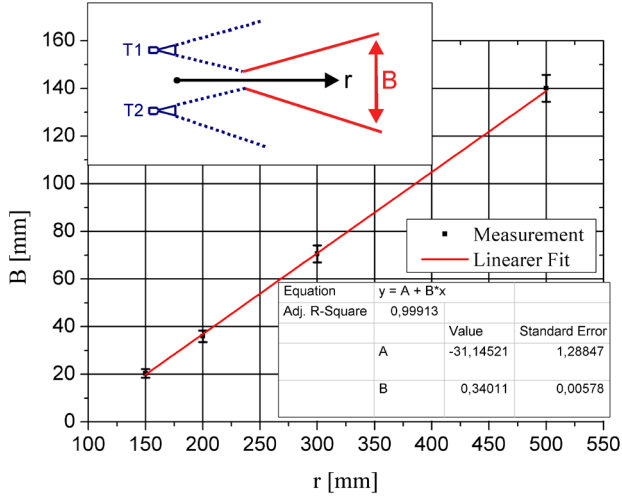


Figure 13. Shock distance B as function of r

Finally we want to check if the limiting Knudsen number $\overline{Kn}_p = 0.2$ for compression wave formation holds also for thruster plume interaction. This knowledge is of practical relevance: If shocks are established the interaction is limited to the region downstream. At $\overline{Kn}_p > 0.2$ the mutual penetration of plume gas becomes more likely the larger \overline{Kn}_p is. As a consequence the interaction region becomes increasingly larger and the effort to determine its properties increases as well. To increase \overline{Kn}_p to this value 0.2 we can either decrease the stagnation pressure p_0 or increase the thruster distance Dy . We show here the results for increasing distance Dy at constant radius $r = 150 \text{ mm}$ in Figure 14 and Figure 15.

All profiles have the same scale for p_K and θ . For completeness we demonstrate in Figure 14 that the shock structure is always visible for $Dy < 30 \text{ mm}$ as expected. The Penetration Knudsen number is depicted for the different profiles. In Figure 15 the change of the shock structure and finally its disappearance is demonstrated. For $Dy = 120$ and $Dy = 170 \text{ mm}$ no shocks are visible. The corresponding Penetration Knudsen numbers are $\overline{Kn}_p = 0.18$ and 0.25 , respectively. A first appearance in this series is observed at $Dy = 72 \text{ mm}$ with $\overline{Kn}_p = 0.11$. The conclusion is that for these thruster plumes a change of the kind of interaction is expected at a \overline{Kn}_p between 0.18 and 0.1. This fits quite well to the result of Dankert and Koppenwallner [3] for free jets. They obtained $\overline{Kn}_p = 0,2$ as limiting Knudsen Number.

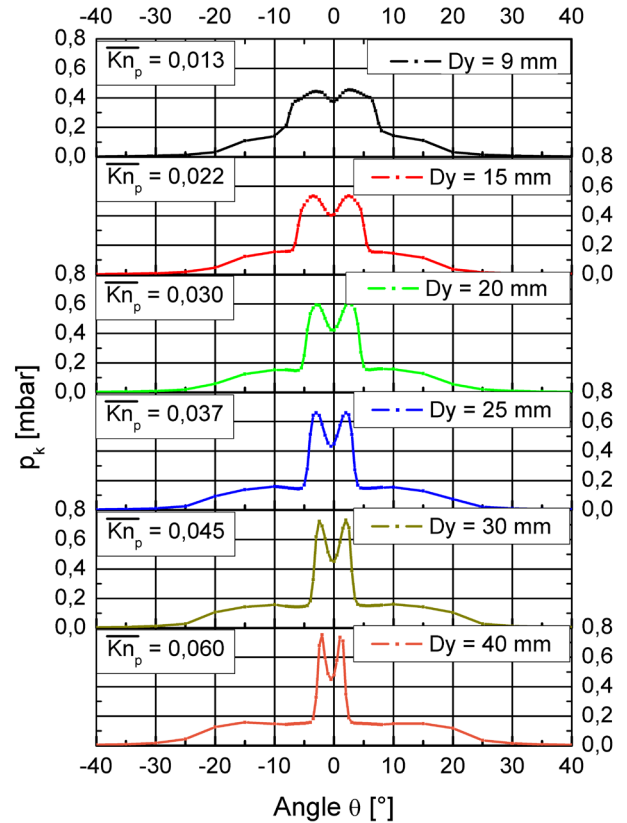


Figure 14. Angular profiles at $r = 150 \text{ mm}$, parameter Dy (Part 1)

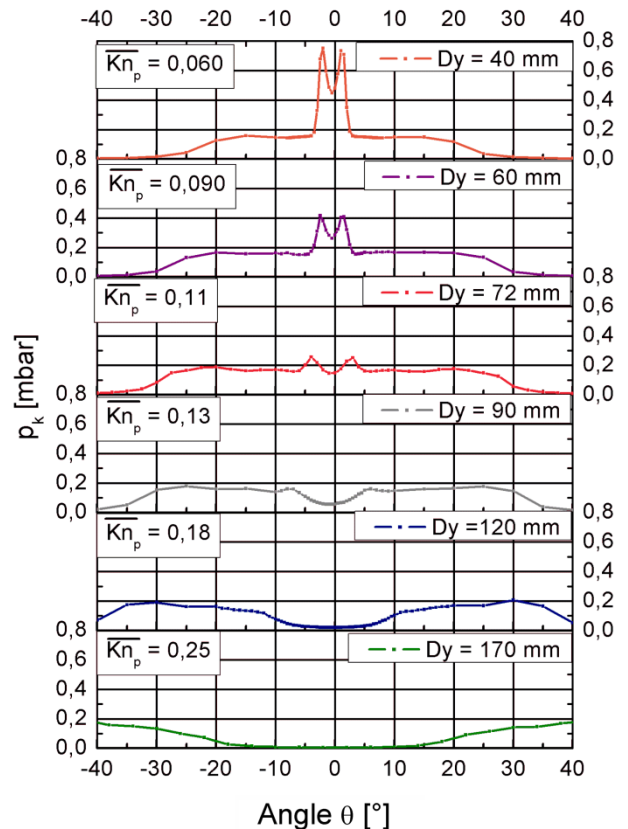


Figure 15. Angular profiles at $r = 150 \text{ mm}$, parameter Dy (Part 2)

4.) Summary and conclusions

In our study of interacting thruster plumes we started with a presentation of some relevant characteristics of the single plume. Details like density distribution and spreading of the core region were presented. This characterization is necessary for further analysis in plume-plume interaction.

The kind of interaction depends on the density in the interaction region and can be characterized by an adapted Knudsen number which is called Penetration Knudsen number Kn_p . It has been shown previously that its value for free jets from sonic orifices indicates if shock interaction is present or not. Here we could show that practically the same characteristic value holds also for thruster plumes with their different angular density distribution. This knowledge is of practical relevance: If shocks are established, the interaction is limited to the region downstream. At $\overline{Kn_p} = 0.2$ the mutual penetration of plume gas becomes more likely the larger $\overline{Kn_p}$ is. As a consequence the interaction region becomes increasingly larger and the effort to determine its properties increases as well.

5.) References

- [1] P. Bley and W. Ehrfeld. Molecular dynamics of disparate mass mixture in opposed jets. In *12th Int. Symp. On Rarefied Gas Dynamics*, 1980.
- [2] C. Dankert and G. Koppenwallner. Experimental study of the interaction between two rarefied free jets. In *14.th Symp. on Rarefied Gas Dynamics, Tokyo*, volume 1, pages 477–484, 1984.
- [3] C. Dankert and G. Koppenwallner. Influence of penetration Knudsen number on interaction of two rarefied free jets. Technical report, DFVLR Göttingen, 1984.
- [4] Georg Dettleff. Plume flow and plume impingement in space technology. *Progress in Aerospace Science*, 28:1–71, 1991.
- [5] Georg Dettleff and Klaus Plähn. Initial experimental results from the new DLR-high vacuum plume test facility STG. In *Proceedings of the 33rd AIAA/ASME/SAE/ASEE Joint Propulsion Conference & Exhibit, AIAA 97-3297, Seattle*, July 6 - 9 1997.
- [6] Georg Dettleff and Klaus Plähn. The new DLR-high vacuum plume test facility STG: Initial acceptance test results. In *Proceedings of the Second European Spacecraft Propulsion Conference, ESA SR-398, Noordwijk*, May 27 - 29 1997.
- [7] F.C. Hurlbut and W. Mc Dermott. Studies of gas mixture separation by opposed jets. In *12th Int. Symp. On Rarefied Gas Dynamics*, 1980.
- [8] G. Koppenwallner. Rarefied plume interference and scaling laws. Interner Bericht IB 222-83 A 27, DFVLR, 1983.
- [9] G. Koppenwallner. The free molecular pressure probe with finite length slot orifice. In *14. th Symposium of Rarefied Gas Dynamics, Tokyo*, 1984.
- [10] G. Koppenwallner. Scaling laws for rarefied plume interference with application to satellite thrusters. In *14th Int. Symp. on Space Technology and Science*, 1984.

- [11] Wenhai Li and Foluso Ladeinde. Simulation and analysis of rarefied parallel interacting sonic jets. In *44th AIAA Aerospace Sciences Meeting and Exhibit, Reno, Nevada*, 2006.
- [12] Klaus Plähn. *Experimentelle Untersuchung und Modellierung von Abgasstrahlen aus Kleintriebwerken in der Kryo-Vakuum-Anlage STG*. Forschungsbericht 1999-39. Deutsches Zentrum für Luft- und Raumfahrt e.V., 1999.
- [13] T. Soga, M. Takanishi, and M. Yasuhara. Experimental study of interaction of underexpanded free jets. In H. Oguchi, editor, *14.th Symp. on Rarefied Gas Dynamics, Tokyo*, pages 485–492, 1984.
- [14] Takeo Soga and Takehiko Hayashi. Numerical analysis of interaction of supersonic free jets, including formation of reverse flow. *Memoirs of the School of Engineering*, 44(2):267–282, March 1993.
- [15] Tecplot, Inc, Post Office Box 52708, Bellevue, WA 98015-2708 USA. *Tecplot. 360 User's Manual*.
- [16] M. Usami, S. Niimi, T. Imura, and T. Takahashi. DSMC calculation of supersonic free jet through a rectangular or a multi-aperture orifice by an improved new collision scheme. In T. Abe, editor, *26.th Symp. on Rarefied Gas Dynamics, Kyoto*, 2009.